

Capillary Experiments of Flow Induced Crystallization of HDPE

Flow-induced crystallization experiments are made in a capillary apparatus modified with a downstream reservoir under pressure. Capillary length, diameter, and entrance angle are changed, as well as flow rate. The results show that the crystallization temperature is influenced both by the elongational flow at the capillary entrance and by the shear flow along the capillary. The independent effect of the pressure equals that obtained under static conditions. The effect of shear is correlated in terms of shearing work.

G. Titomanlio

Dipartimento di Ingegneria Chimica dei
Processi e dei Materiali
Viale delle Scienze
90128 Palermo, Italy

G. Marrucci

Dipartimento di Ingegneria Chimica
Piazzale Tecchio
80125 Napoli, Italy

Introduction

Flow-induced crystallization of polymers has been known for a long time and its importance in polymer processing is well recognized. Generally, the influence of flow is that of enhancing the rate of crystallization as well as that of changing the morphology of the crystalline material. Review papers on this subject are available, see, e.g., McHugh (1982) and Pucci and Carr (1983) for the cases of solutions and melts, respectively.

Although these phenomena are understood in their general aspects, several questions still remain open, among them the relative effectiveness, in promoting crystallization, of elongational flows vs. shear flows, or the possible synergistic effect of a high pressure superposed to flow.

By using a capillary apparatus, Southern and Porter (1970) obtained results indicating that, in the conditions of their experiment, high-density polyethylene (HDPE) crystallization occurred at the entrance of the capillary. This was attributed to the combined effect of the pressure and of the converging flow upstream of the capillary, which is mainly elongational. On the other hand, it is known that HDPE also undergoes premature crystallization by applying a shear flow. The results of Tan and Gogos (1976) provide a good description of the effect. They show that, whereas the incubation time for crystallization depends on both temperature and shear rate, the work done during the incubation time depends only on temperature. Thus a work criterion suggests itself as a possible basis for quantitative predictions.

In this work, we have further investigated the behavior of HDPE in the capillary apparatus. In particular, we have used capillaries of various lengths so as to change the relative importance of shear with respect to elongation. Also, since by changing the length of the capillary the pressure inevitably varies, we

have independently investigated the pressure effect by generating an additional pressure drop downstream of the main capillary.

Experimental Studies

The experiments were run in a capillary rheometer (Rheoscope 1000, manufactured by CEAST) modified as shown in Figure 1. A downstream reservoir is used, which allows a higher pressure to be set at the exit of the main capillary. The reservoir is pressurized by means of the flow through a secondary capillary. Preliminary measurements of the pressure drop through the set of secondary capillaries were made, by using the same polymers, so as to predetermine the pressure in the downstream reservoir during the main experiments.

In order to avoid crystallization in the secondary capillary, the temperature of the downstream reservoir was held fixed at 160°C, i.e., sufficiently above the quiescent crystallization temperature. The additional reservoir could be easily disconnected when data under standard conditions were to be taken.

The length of the main capillaries ranged from 5 to 60 mm. Two values of diameter were used, i.e., 1.0 and 1.5 mm. The polymer was fed to the main capillary from a cylindrical reservoir, ca. 10 mm dia. In most experiments, the entrance angle to the capillary was 180°; in a few cases, however, a conical entrance with a 90° angle was used. The polymer was fed by means of a piston. The piston velocities which were used systematically in this work were .5 and 2.0 mm/min, though occasional data at 5.0 mm/min were also taken.

In a typical experimental run, the temperature of the upstream reservoir was initially set at 180°C and then progressively decreased. After each temperature step, a sufficiently long time (ca. 30 min) was allowed for achieving a good temper-

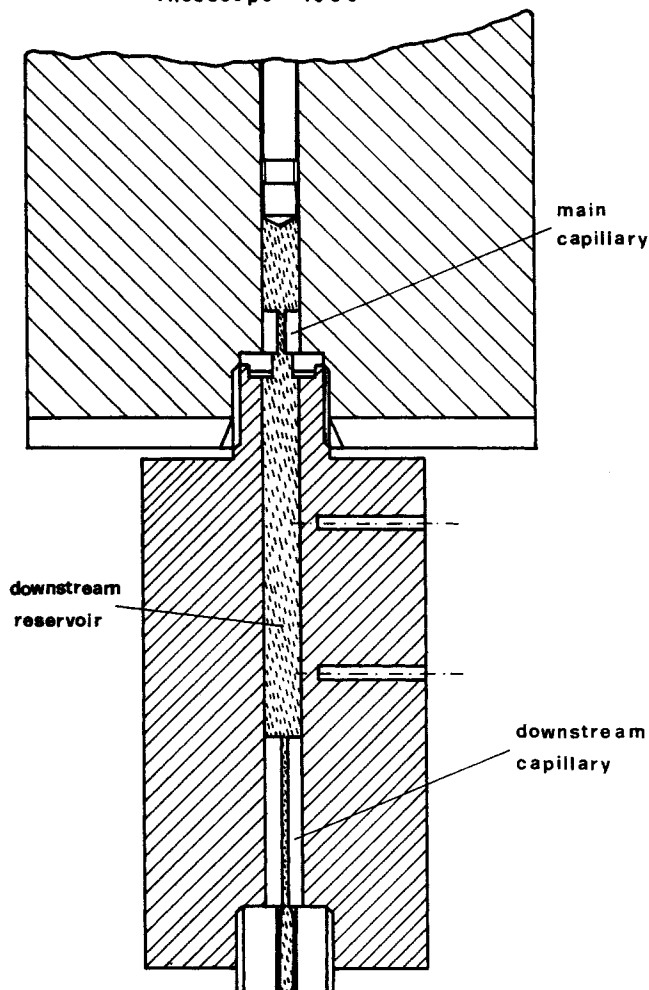


Figure 1. Modified capillary apparatus.

ature uniformity. At all temperatures during each run, the flow was started, always with the same value of the piston velocity, and the force acting on the piston was recorded. With decreasing the temperature, the force first increased weakly, then more rapidly, and finally abruptly, beyond the machine limits. Under these conditions, the flow stopped, and the run obviously ended. The temperature corresponding to this event is indicated as T_c .

Data such as those just described were obtained for all capillaries and flow rates previously mentioned, with and without the additional reservoir. In order to vary the exit pressure, a set of secondary capillaries was used, calibrated as mentioned above. Two grades of HDPE were used, having M_w at approximately 113,000 and 395,000, called samples *B* and *F*, respectively. For a characterization of these polymers, we refer to the work of La Mantia et al. (1983).

For some runs, once T_c had been reached, the apparatus was cooled down to room temperature while maintaining the maximum force on the piston, and the polymer within the main capillary was then recovered. Following the same procedure adopted by Southern and Porter (1970), differential scanning calorimetry (DSC) tests (heating rate = 10°C/min) were performed on small sections, cut at different locations of the cylindrical specimen, i.e., corresponding to well defined locations along the capillary.

It should finally be mentioned that the quiescent crystallization temperature, T_m , was determined, for both samples *B* and *F*, by DSC under both cooling and heating conditions, at several cooling and heating rates. T_m is obtained from the limiting values at zero rate of both the initial crystallization and the final melting temperatures. We obtained $T_m = 127^\circ\text{C}$ and $T_m = 129^\circ\text{C}$ for samples *B* and *F*, respectively.

Results and Discussion

Figure 2 shows typical curves of the pressure upstream of the main capillary as a function of temperature. The pressure values are obtained by dividing the recorded force by the piston cross section. All curves in Figure 2 refer to the same value of the capillary diameter and to the same flow rate. The polymer is sample *F*, and the exit pressure is atmospheric, i.e., the additional reservoir is disconnected. In this case, of course, the pressure in the main reservoir coincides with the pressure drop across the main capillary.

As previously mentioned, these curves show an abrupt upturn at a critical temperature, T_c . Similarly to what is done by Southern and Porter (1970), the upturn is interpreted as due to flow-induced crystallization. This interpretation is further supported by the behavior of the die swell effect, reported in Figure 3. Whereas at higher temperature the die swell ratio, DS , attains typical values for molten polymers, abnormally large values are observed at temperatures close to T_c , indicating a larger melt elasticity due to some form of aggregation.

It should be noted that the values of T_c shown in Figure 2 are considerably larger than the quiescent crystallization temperature ($T_m = 129^\circ\text{C}$ for sample *F*). Even larger effects are found at larger flow rates. Figure 2 shows that T_c increases significantly with increasing capillary length.

Figure 4 refers to the case when the downstream reservoir is used. The lower curve in Figure 4, taken from Figure 2, is used for comparison. All curves in Figure 4 are obtained with the same main capillary, whereas the secondary one is changed so as to obtain different pressure levels. Figure 4 shows that raising the pressure level while maintaining the same pressure drop in the main capillary, has a relatively minor effect on T_c . As fur-

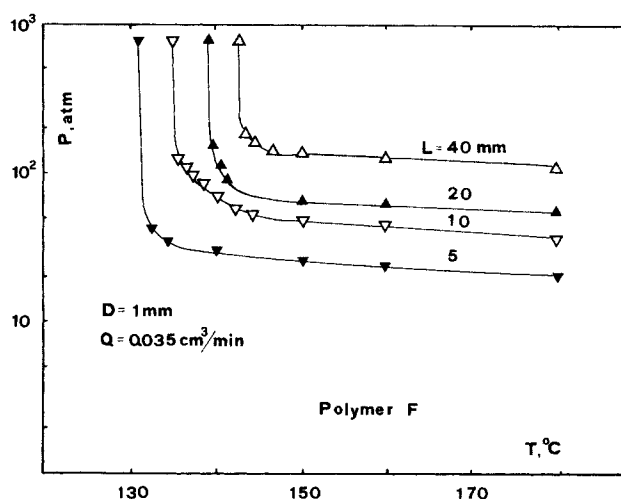


Figure 2. Pressure in the upstream reservoir vs. temperature: effect of capillary length.

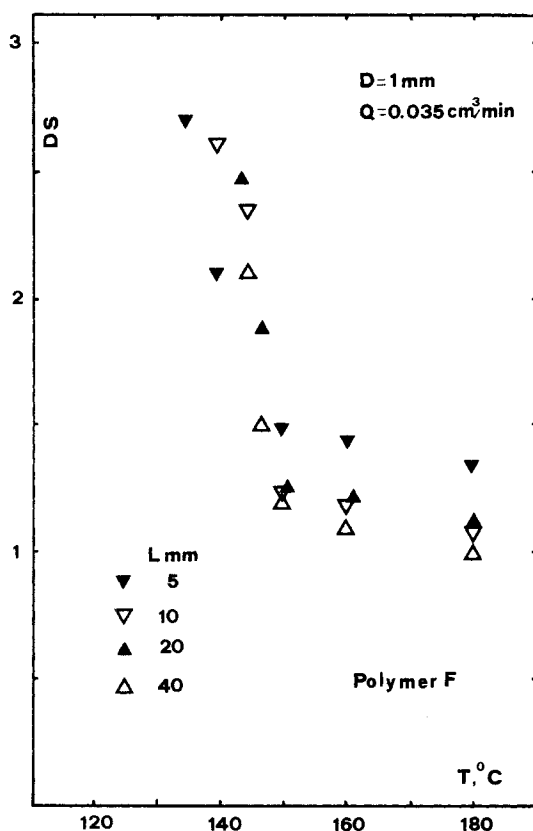


Figure 3. Die swell ratio measured on the solid extrudate vs. temperature.

ther discussed later in the paper, the effect observed here merely coincides with the pressure effect under static conditions.

Figures 5–7 show the influence of flow rate, capillary diameter, and entrance angle, respectively. The anomalous behavior of the upper curve in Figure 5, i.e., the dip in the curve, is due to the onset of an instability which, however, was limited to a small temperature range. To avoid possible complications, in all other experiments the values of the shear rate were kept below that corresponding to the upper curve in Figure 5. As expected, Figure 5 shows that T_c increases with increasing flow rate Q .

Figure 6 reports some results obtained with the 1.5 mm capillary diameter. It is not immediately evident how to compare these results with those in Figure 2 and 5, i.e., which parameters

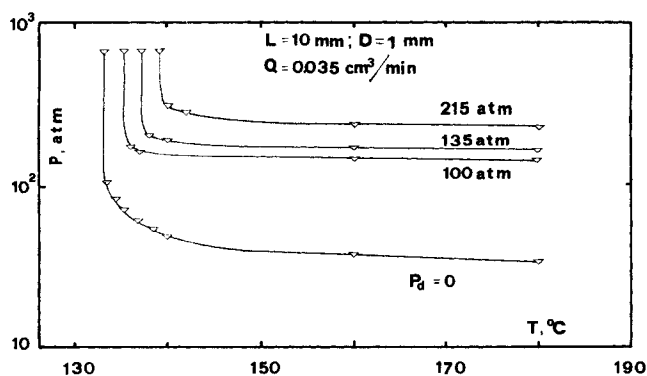


Figure 4. Pressure vs. temperature in the upstream reservoir: effect of downstream pressure, P_d .

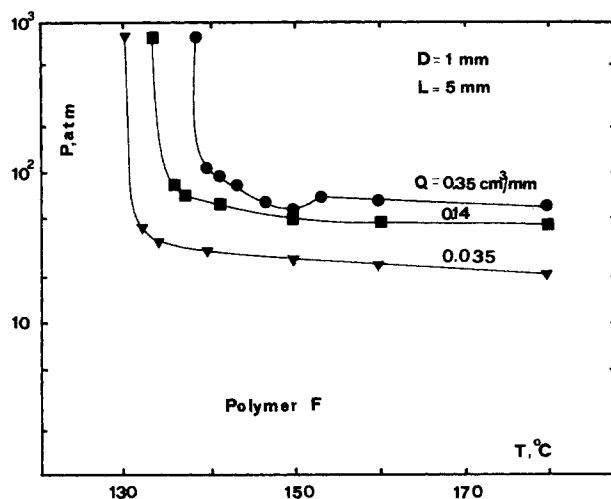


Figure 5. Pressure vs. temperature in the upstream reservoir: effect of flow rate.

to hold fixed in the comparison. It is observed, however, that all values of T_c in these figures are ordered according to the pressure drop in the capillary. More precisely, when the pressure drop (evaluated before crystallization begins, i.e., at high T) increases, the value of T_c correspondingly increases. We will further discuss this point in the following.

Finally, Figure 7 shows the influence of the entrance angle. There is no doubt that a conical entrance gives rise to smaller values of T_c than the flat entrance.

All results for polymer F are reported in Figure 8 as T_c vs. P_r , the pressure in the upstream reservoir measured at a reference temperature of 160°C, i.e., well above the highest T_c observed. The dashed straight line in Figure 8 starts from T_m , at $P_r = 0$, and has a slope of 0.022°C/atm. It represents the increase in crystallization temperature with pressure, under static conditions. Parallel straight lines are drawn through two sets of data, each of them obtained with the same primary capillary and flow rate, the pressure level being changed by using the downstream reservoir. Conversely, the two curves in Figure 8 refer to the

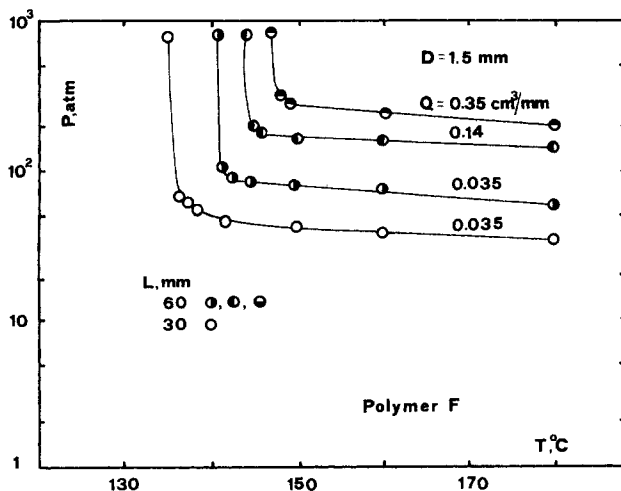


Figure 6. Pressure vs. temperature in the upstream reservoir. Results obtained with the 1.5-mm-dia. capillary.

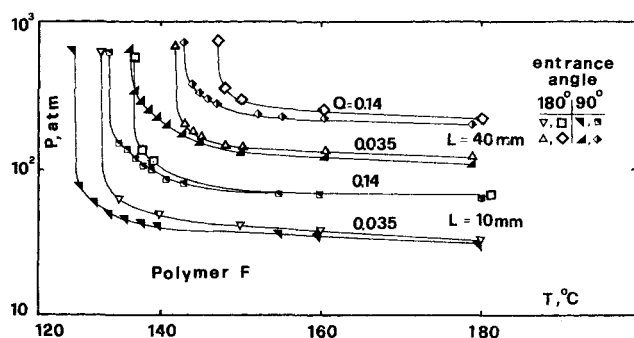


Figure 7. Pressure vs. temperature in the upstream reservoir: effect of entrance angle.

data obtained without the downstream capillary, i.e., with an atmospheric exit. The upper curve collects the results for the flat entrance case, whereas the lower one refers to the conical entrance.

It should be noted that, for each kind of entrance separately, all data correlate quite nicely with the pressure drop in the primary capillary, independently of the way that pressure drop was obtained, i.e., if by varying the flow rate, or the capillary length, or the capillary diameter. Indeed, the data obtained with the atmospheric exit are already grouped along the curves in Figure 8. As far as the other data are concerned, those along each straight line in Figure 8 would virtually collapse into a single point once the pressure drop instead of the absolute pressure is considered, and the static pressure effect is accounted for. With regard to the latter effect, the value previously indicated, of $0.022^{\circ}\text{C}/\text{atm}$, was evaluated in the course of this work from free cooling experiments under pressure, and favorably compares with literature data (see, e.g., Sandiford and Willbourn, 1960).

Similar results were obtained with polymer B. These are summarized in Figure 9 where, again, T_c vs. P is reported. In this case, a single curve correlates all data. In fact, for polymer B, we

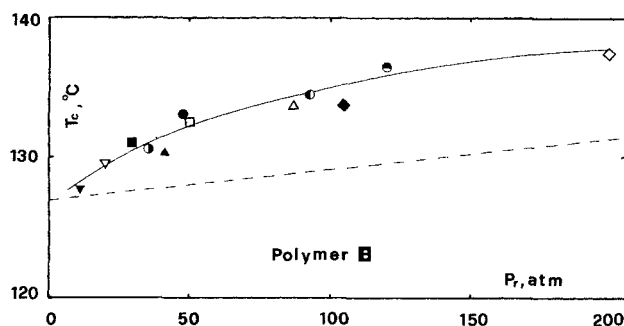


Figure 9. Critical temperature vs. reference pressure for polymer B.

Key to symbols as in Figure 8.

never used the conical entrance or the downstream reservoir. It should be noted that, since polymer B has a lower molecular weight than polymer F, a reduced influence of flow on crystallization is observed. This is apparent in the smaller values of $T_c - T_m$ which, at equal P , are found for this polymer.

Figure 10 reports some of the DSC graphs which were obtained from sections of the samples, solidified as previously described. The graphs to the left of the figure show essentially a single peak at a high temperature, corresponding to highly oriented material. Conversely, those to the right show a bimodal structure, indicating the coexistence of different kinds of crystals. Notice that, since the sections contain material close to the capillary wall together with material close to the axis, it is not clear whether the two peaks originate from a local mixture of different crystalline material or from materials located at different radial positions.

The change observed in the DSC results along the axis of the capillary is a complex one, and varies considerably with the operating conditions. Figure 11 reports the peak temperature of the more oriented material, T_p , as a function of the distance from the capillary inlet, z . The data refer to two values of the

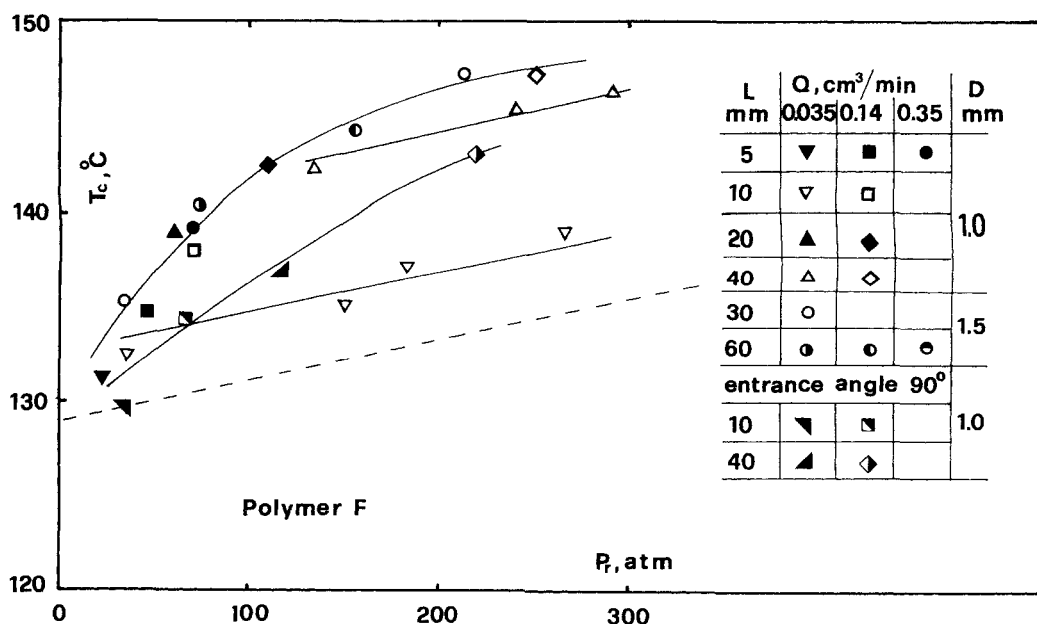


Figure 8. Critical temperature vs. reference pressure. All results obtained with polymer F are reported.

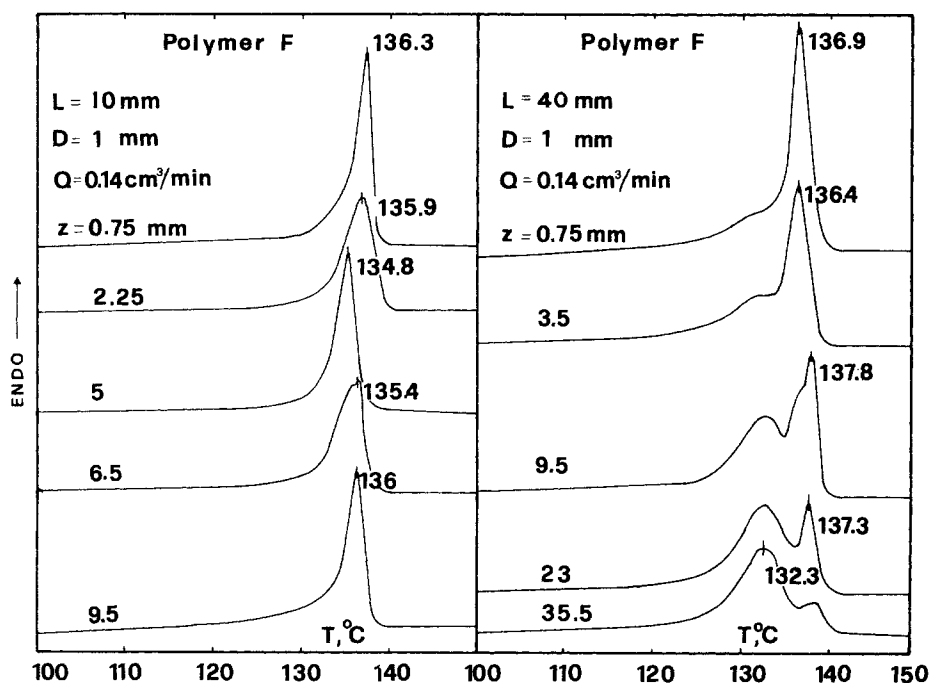


Figure 10. DSC results for short and long capillaries.

The distance, z , from capillary inlet is indicated.

capillary length and two values of the flow rate. The following considerations can be made. Only in one case, i.e., for the case of the short capillary at a low flow rate, T_p decreases monotonically with increasing z . In all other cases, T_p first decreases somewhat, then increases again, sometimes up to larger values than that at $z = 0$, and finally decreases again (or it remains essentially constant). For the longer capillary, which shows bimodal DSC curves, the behavior of the lower temperature peak as a function of z can also be analyzed. It is found that this temperature also slightly decreases, or stays constant, with increasing z .

The fact that T_p often shows a maximum at some location along the capillary suggests that the shearing taking place within the capillary plays a significant role in the crystallization process. Indeed, should the flow stop (at $T = T_c$) as a consequence of massive solidification at the entrance of the capillary (because of the elongational flow upstream), then T_p would be found always decreasing with increasing z . The argument here

is the same as that used by Southern and Porter (1970) to explain their data, i.e., the polymer downstream, now stagnant, either melts again, because of the reduced pressure, or was already in the molten state before cessation of flow. In either event, when it solidifies by cooling down the apparatus, it certainly cannot generate crystalline material with higher melting points. Conversely, the DSC results obtained in this work indicate that massive crystallization takes place at some place along the capillary, rather than at the entrance. It so appears that the shear flow provides a significant contribution, which adds to that of the previous elongational flow.

The above conclusion about the relevance of the shear contri-

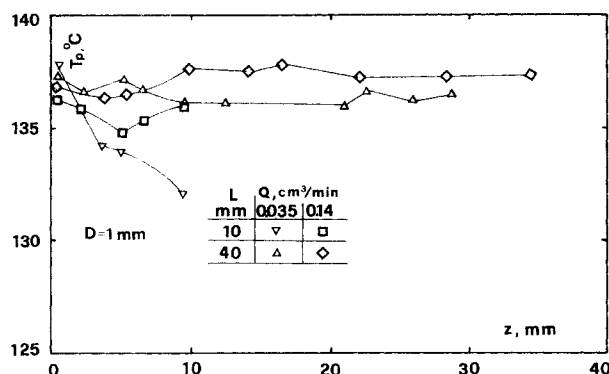


Figure 11. High-temperature DSC peaks vs. the distance from capillary inlet.

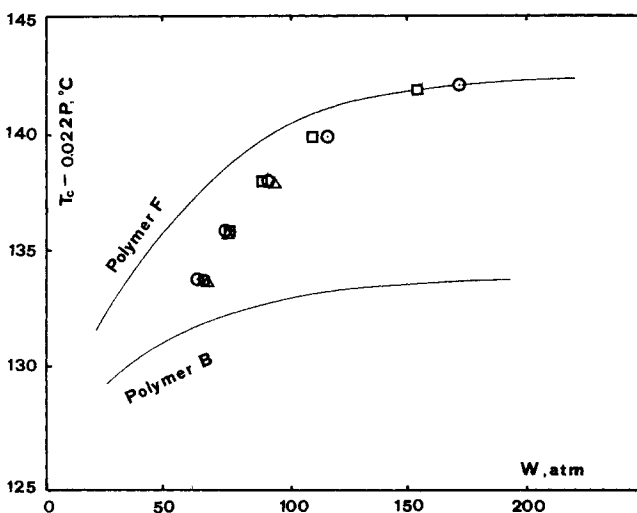


Figure 12. Critical temperature vs. shearing work.

Curves, corrected for the static pressure effect, are from Figures 8 and 9. Data from Tan and Gogos for several shear rates: $\square = 7.575 \text{ s}^{-1}$, $\circ = 3.030 \text{ s}^{-1}$, and $\triangle = 1.515 \text{ s}^{-1}$.

bution is confirmed by the T_c dependence on capillary length. The fact that T_c increases with increasing the length of the capillary cannot be explained in terms of a pressure effect (see previous discussion of Figures 4 and 8). The possible explanation is that the shear makes the crystals to grow along the capillary.

Conclusions

The results obtained in this work show that flow-induced crystallization in a capillary is a complex phenomenon where both the elongational flow at the entrance and the shear flow along the capillary play a substantial role. The elongational contribution, already stressed by Southern and Porter (1970), appears explicitly from the comparison between the results obtained with different entrance angles, since changing the geometry of the entrance to the capillary mainly affects the elongational flow upstream. The shear contribution is apparent when examining the dependence of T_c on the capillary length or that of T_p on the distance from the entrance.

No synergistic effect of the pressure *per se* has been found. When the pressure level is raised by means of the downstream reservoir, T_c only increases according to thermodynamics, i.e., in the same way as under static conditions.

The fact that all values of T_c obtained under different conditions show a good correlation with the pressure drop in the capillary deserves further comment. It is noted that the pressure drop coincides with the work (per unit volume) done on the material. Thus, similar to the results obtained by Tan and Gogos (1976) with a biconical apparatus, we find that the shearing work required to reach crystallization at a given temperature depends only on the temperature itself. With the capillary apparatus, however, the complication of the elongational flow at the entrance makes the correlation dependent on the inlet geometry as well.

The data reported in Table 1 of the paper of Tan and Gogos (1976) for an HDPE of $M_w = 140,000$ are plotted in Figure 12. The curves in the same figure are taken from Figures 8 and 9 of this paper, for the case of a flat entrance. Since the biconical apparatus of Tan and Gogos is obviously atmospheric, the curves in Figure 12 report the value of $T_c - 0.022 P$, rather than T_c , so as to correct for the static pressure effect in the capillary.

It is noted that the curves and the data of Tan and Gogos have similar shapes. In both cases, there is a clear tendency toward a saturation of the effect of the shearing work, W , on the flow-induced crystallization temperature as W increases.

Acknowledgment

Work supported by Ministero della Pubblica Istruzione, Rome.

Notation

- D = capillary diameter
- DS = die swell ratio
- L = capillary length
- M_w = weight average molecular weight
- P = pressure in the upstream reservoir
- P_d = pressure in the downstream reservoir
- P_u = pressure in the upstream reservoir at 160°C
- T = temperature in the rheometer
- T_c = temperature at which pressure drop undergoes an abrupt increase
- T_m = normal crystallization temperature under quiescent conditions at atmospheric pressure
- T_p = peak temperatures in DSC thermograms
- W = work per unit volume inducing crystallization in the polymer
- z = distance from capillary inlet

Literature Cited

- La Mantia, F. P., A. Valenza, and D. Acierno, "A Comprehensive Experimental Study of the Rheological Behavior of HDPE: I. Entrance Effects and Shear Viscosity Results," *Rheol. Acta*, **22**, 299 (1983).
- McHugh, A. J., "Mechanics of Flow-Induced Crystallization," *Polym. Eng. Sci.*, **15**, 22 (1982).
- Pucci, M. S., and S. H. Carr, "Crystal Nucleation in Flowing Polymer Melts," *Polym. Sci. Technol.*, **22**, Plenum (1983); *Struct.-Prop. Relat. Polym. Solids*, 139.
- Sandiford, D. J. H., and A. H. Willbourn, "General Mechanical Properties," *Polythene*, Eds., A. Refrew and P. Morgan, Interscience, New York (1960).
- Southern, J. H., and R. S. Porter, "Polyethylene Crystallized Under the Orientation and Pressure of a Pressure Capillary Viscometer: Part I," *J. Macromol. Sci.-Phys.*, **B4**(3), 541 (1970).
- Tan, V., and C. Gogos, "Flow-Induced Crystallization of Linear Polyethylene Above its Normal Melting Point," *Polym. Eng. Sci.*, **16**, 510 (1976).

Manuscript received June 19, 1989, and revision received Sept. 28, 1989.